



Deposited via The University of Leeds.

White Rose Research Online URL for this paper:

<https://eprints.whiterose.ac.uk/id/eprint/186536/>

Version: Accepted Version

Article:

Hastie, A, Honorio Coronado, EN, Reyna, J et al. (2022) Risks to carbon storage from land-use change revealed by peat thickness maps of Peru. *Nature Geoscience*, 15. pp. 369-374. ISSN: 1752-0894

<https://doi.org/10.1038/s41561-022-00923-4>

© Crown 2022. This is an author produced version of an article, published in *Nature Geoscience*. Uploaded in accordance with the publisher's self-archiving policy.

Reuse

Items deposited in White Rose Research Online are protected by copyright, with all rights reserved unless indicated otherwise. They may be downloaded and/or printed for private study, or other acts as permitted by national copyright laws. The publisher or other rights holders may allow further reproduction and re-use of the full text version. This is indicated by the licence information on the White Rose Research Online record for the item.

Takedown

If you consider content in White Rose Research Online to be in breach of UK law, please notify us by emailing eprints@whiterose.ac.uk including the URL of the record and the reason for the withdrawal request.

1 Risks to carbon storage from land-use change revealed by peat thickness maps of 2 Peru

3 Adam Hastie¹, Eurídice N. Honorio Coronado^{2,3}, José Reyna³, Edward T. A. Mitchard¹, Christine M.
4 Åkesson², Timothy R. Baker⁴, Lydia E. S. Cole², César. J. Córdova Oroche³, Greta Dargie⁴, Nállarett
5 Dávila³, Elsa Carla De Grandi¹, Jhon Del Águila³, Dennis Del Castillo Torres³, Ricardo de la Cruz
6 Paiva⁵, Frederick C. Draper^{4,6}, Gerardo Flores³, Julio Grández³, Kristell Hergoualc'h⁷, J. Ethan
7 Householder⁸, John P. Janovec⁹, Outi Lähteenoja¹⁰, David Reyna³, Pedro Rodríguez-Veiga^{11,12},
8 Katherine H. Roucoux², Mathias Tobler¹³, Charlotte E. Wheeler^{1,7}, Mathew Williams^{1,14}, Ian T.
9 Lawson².

10 Affiliations

11 1 School of GeoSciences, University of Edinburgh, Edinburgh, United Kingdom
12 2 School of Geography and Sustainable Development, University of St Andrews, St Andrews, United Kingdom
13 3 Instituto de Investigaciones de la Amazonía Peruana (IIAP), Av. Abelardo Quiñonez km 2.5, Iquitos, Perú
14 4 School of Geography, University of Leeds, Leeds, United Kingdom
15 5 Servicio Nacional Forestal y de Fauna Silvestre, Avenida Javier Prado Oeste, Magdalena del Mar, Lima, Perú
16 6 Center for Global Discovery and Conservation Science, Arizona State University, AZ, United States of America
17 7 Center for International Forestry Research (CIFOR), Jl. CIFOR, Situ Gede, Bogor, 16115, Indonesia
18 8 Wetland Ecology, Institute for Geography and Geoecology, Karlsruhe Institute for Technology, Karlsruhe, Germany
19 9 Sam Houston State University Natural History Museum, Sam Houston State University, Huntsville, TX, USA
20 10 Helsinki, Finland
21 11 Centre for Landscape and Climate Research (CLCR), School of Geography, Geology and Environment, University of
22 Leicester, University Road, Leicester LE1 7RH, UK
23 12 National Centre for Earth Observation, University of Leicester, Space Park Leicester, Corporation Road, Leicester LE4
24 5SP, UK
25 13 San Diego Zoo Global, Institute for Conservation Research, 15600 San Pasqual Valley Road, Escondido, CA, USA
26 14 NCEO, University of Edinburgh, UK

27

28 Abstract

29 Tropical peatlands are among the most carbon dense ecosystems but land-use change has
30 led to the loss of large peatland areas, associated with substantial greenhouse gas
31 emissions. In order to design effective conservation and restoration policies, maps of the
32 location and carbon storage of tropical peatlands are vital. This is especially so in countries
33 such as Peru where the distribution of its large, hydrologically intact peatlands is poorly
34 known. Here, field and remote sensing data support model development of peatland extent
35 and thickness for lowland Peruvian Amazonia. We estimate a peatland area of 62,714 (5th
36 and 95th confidence interval percentiles 58,325–67,102 respectively) km² and carbon stock
37 of 5.4 (2.6–10.6) Pg C, a value approaching the entire above-ground carbon stock of Peru
38 but contained within just 5% of its land area. Combining the map of peatland extent with
39 national land-cover data we reveal small but growing areas of deforestation and associated
40 CO₂ emissions from peat decomposition, due to conversion to mining, urban areas, and

41 agriculture. The emissions from peatland areas classified as forest in 2000 represent 1–4%
42 of Peruvian CO₂ forest emissions between 2000 and 2016. We suggest that bespoke
43 monitoring, protection and sustainable management of tropical peatlands are required to
44 avoid further degradation and CO₂ emissions

45 **Main text**

46 While tropical peatlands are known to be among the most carbon-dense ecosystems in the
47 tropics^{1,2}, their absolute contribution to the global carbon cycle remains highly uncertain,
48 with recent estimates placing their total below-ground carbon storage between 105 (70–
49 130) and 215 (152–288) Pg C^{3,4}. They face various threats including land-use and climate
50 change^{4,5}. Deforestation and/or drainage of peatlands inhibit the accumulation of organic
51 matter and promotes rapid decomposition of peat, releasing large quantities of the
52 greenhouse gasses (GHG) CO₂ and N₂O to the atmosphere^{6,7,8,9,10}. Moreover, drained
53 peatlands are prone to fires which lead to large pulses of emissions¹¹. The experience of
54 Indonesia provides a cautionary tale: in 1997 alone, it was estimated that between 0.81 and
55 2.57 Pg C were released as a result of peat and vegetation fires, which at the time equated
56 to 13–40% of global fossil fuel emissions¹². Indeed, the peatlands of Southeast Asia have
57 already been severely damaged with almost 80% cleared and drained¹³. In contrast, the
58 largest known peatland areas in tropical Africa and South America are thought to remain
59 largely intact^{14,15}.

60 As such, commitments to avoid further deforestation and degradation by 1) promoting
61 conservation and sustainable management of intact peatlands and 2) restoring degraded
62 peatlands, are essential to reducing CO₂ emissions and avoiding global warming of 1.5°C or
63 more^{16,17}. A funding mechanism for this is potentially offered by UNFCCC initiatives,
64 including REDD+ and wider National Determined Contributions¹⁸ to the Paris Agreement,

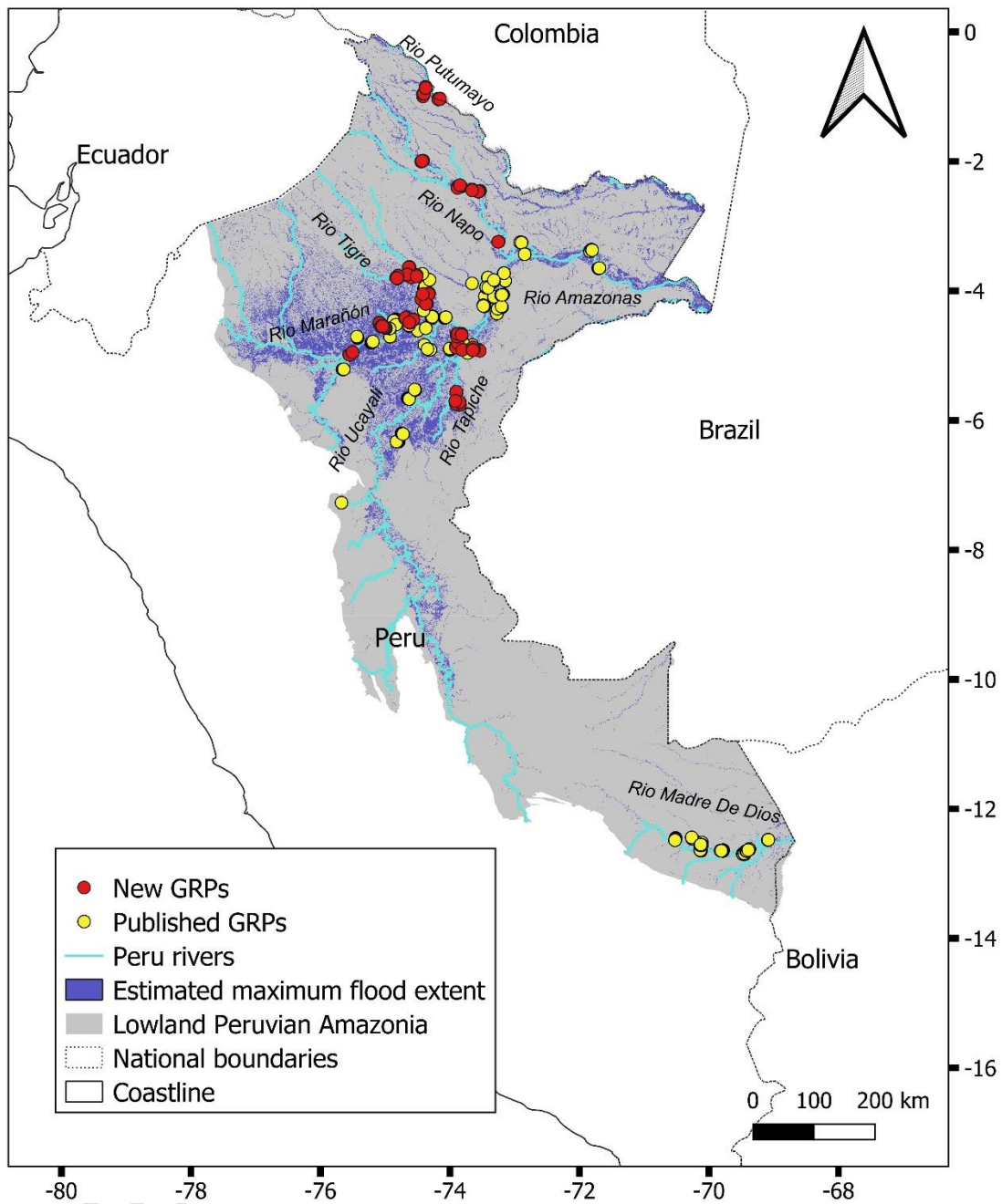
65 but a necessary first step towards conservation and restoration is reliable mapping of the
66 spatial distribution of peatlands and their carbon stocks, at scales relevant to the
67 development of national policies.

68 Peru has substantial known regions of hydrologically intact peatland. Previous research
69 identified a large area in the Pastaza-Marañón Foreland Basin in northern Peru (PMFB, Fig.
70 S1), estimating its carbon stock to be 3.14 (0.44–8.15) Pg C including above- and below-
71 ground carbon², and a smaller area in the Madre de Dios (MDD) region of southern Peru
72 holding an estimated 0.03 Pg C¹⁹). However, published wetland maps^{20,21} and visual
73 examination of remote sensing imagery suggest that there are likely other significant
74 peatlands in Peru whose carbon stocks remain unquantified. Even in the best-known region,
75 the PMFB, previous mapping was based on relatively small numbers of peat thickness
76 measurements and did not attempt to model and map the spatial variation in peat
77 thickness^{2,22}, one of the greatest sources of uncertainty in the below-ground carbon stock².
78 Rather, the total below-ground carbon stock for the PMFB was estimated by determining
79 the area of different peat-forming vegetation classes (i.e. peatland pole forest, palm swamp
80 and open peatland) and multiplying those areas by a mean below-ground carbon stock for
81 each vegetation class. This approach makes several simplifying assumptions²³: that these
82 three vegetation classes are always underlain by peat, that peat thickness varies more
83 between than within classes, and that other landcover classes (including some wetland
84 ecosystems such as seasonally flooded forest) never overlie peat^{2,22}. In fact, field
85 observations indicate that these assumptions are no longer valid; in particular, peat
86 thickness varies substantially in space, including within single vegetation classes^{3,23}. Data-
87 driven maps that more accurately capture the spatial variation in peat thickness and carbon

88 storage, and that cover not just selected study areas but the whole of Peruvian Amazonia,
89 are required to support national and regional peatland conservation planning.

90 While Peruvian peatlands are believed to remain largely intact, thus far there has been no
91 quantitative assessment of GHG emissions resulting from landcover change. Moreover, they
92 face varied and increasing threats including agriculture expansion, illegal mining, oil
93 exploration, infrastructure development, and the selective felling of the female *Mauritia*
94 *flexuosa* palm for commercial purposes^{15,23,24,25,26}. In recognition of these threats, legislation
95 has recently been enacted which, for the first time, mandates the explicit protection of
96 peatlands in Peru for climate-change mitigation²⁷. Enforcing this legislation effectively will
97 depend on robust mapping of peatland distribution, and on knowledge of the scale and
98 distribution of recent peatland disturbance, none of which is presently available.

99 Here we present extensive new field observations (Fig. 1) to test whether previous evidence
100 of a relationship between distance to peatland edge and peat thickness found in other
101 tropical peatlands³, also applies in Peru. These data are used along with remote sensing
102 imagery to develop the first data-driven models of peatland extent and peat thickness
103 distribution across the whole of lowland Peruvian Amazonia (LPA). We quantify the spatial
104 variation and total peat carbon stock of these peatlands, and associated uncertainties.
105 Finally, we use these models, along with national data on land-cover change, to map
106 peatland disturbance and estimate the associated CO₂ emissions for the period 2000–2016.



107

108 **Figure 1: Distribution of the 1,128 ground reference points (GRPs) sampled for peat thickness and**
 109 **vegetation type data used in this study.** The points include GRPs collected from 2019-2021 as part
 110 of this study (red, n = 445) as well as published GRPs from^{2,19,22,28} (yellow). Estimated maximum flood extent
 111 is derived from the wetlands map of ref.²⁰. Rivers of Strahler order ≥ 6 are shown.

112

113

114

115 ***Peat thickness distribution reveals a large carbon store***

116 We estimate a total peatland extent of 62,714 (58,325–67,102) km² (Fig. S2), a mean peat
117 thickness of 203 (179–224) cm (Fig. 2, Fig. S3) and a total below-ground carbon stock of 5.38
118 (2.55–10.58) Pg C (Fig. S4) across the LPA. In addition to the well-known peatlands of the
119 PMFB and MDD basin, we identify substantial areas of peatland in the Ucayali (11,110 km²;
120 2,258 km in Tapiche sub-basin), Napo (3,670 km²) and Putumayo (2,319 km²) basins (Fig. 2,
121 Fig. S1, Table S1). Palm swamp is the most extensive peat-forming ecosystem (46,423 km²)
122 and therefore contains the greatest stock (3.83 Pg C), despite pole forest and open peatland
123 having higher peat carbon densities (1,054 Mg C ha⁻¹ and 1,061 Mg C ha⁻¹ respectively, Table
124 S2). We estimate that 2% of seasonally flooded forest overlies peat, equating to an area of
125 1,951 km² and a peat C stock of 0.11 Pg C (Table S2).

126 The distribution of peat thickness across the LPA is highly variable, with the greatest mean
127 peat thickness predicted in the Tigre (232 cm), Marañón (230 cm), Tapiche (234 cm), and
128 Napo basins (223 cm) (Fig. 2, Table S1). Our models of peatland area and peat thickness
129 distribution performed well against observations (Table S3, Fig. S5), giving confidence in our
130 results. We ran two separate peat thickness models: one for the MDD basin and another for
131 all the rest of the study area (which contains 97% of total peatland area). The model which
132 excluded the MDD basin performed better ($p < 0.0001$; $R^2 = 0.66$, RMSE = 66%, Fig. S5a)
133 than the MDD model ($p < 0.0001$; $R^2 = 0.38$, RMSE = 70%, Fig. S5b). We found a significant
134 linear relationship between peat thickness and distance to peatland edge ($p < 0.0001$, $R^2 =$
135 0.13, Fig. S6a). This relationship was more significant when the data from the MDD basin
136 were excluded (giving $R^2 = 0.39$, $p < 0.0001$, Fig. S6b) and there was no significant

137 relationship between peat thickness and distance to peatland edge within the MDD data (p
138 > 0.1 , $R^2 = 0.005$, Fig. S6c).

139

140

141

142

143

144

145

146

147

148

149

150

151

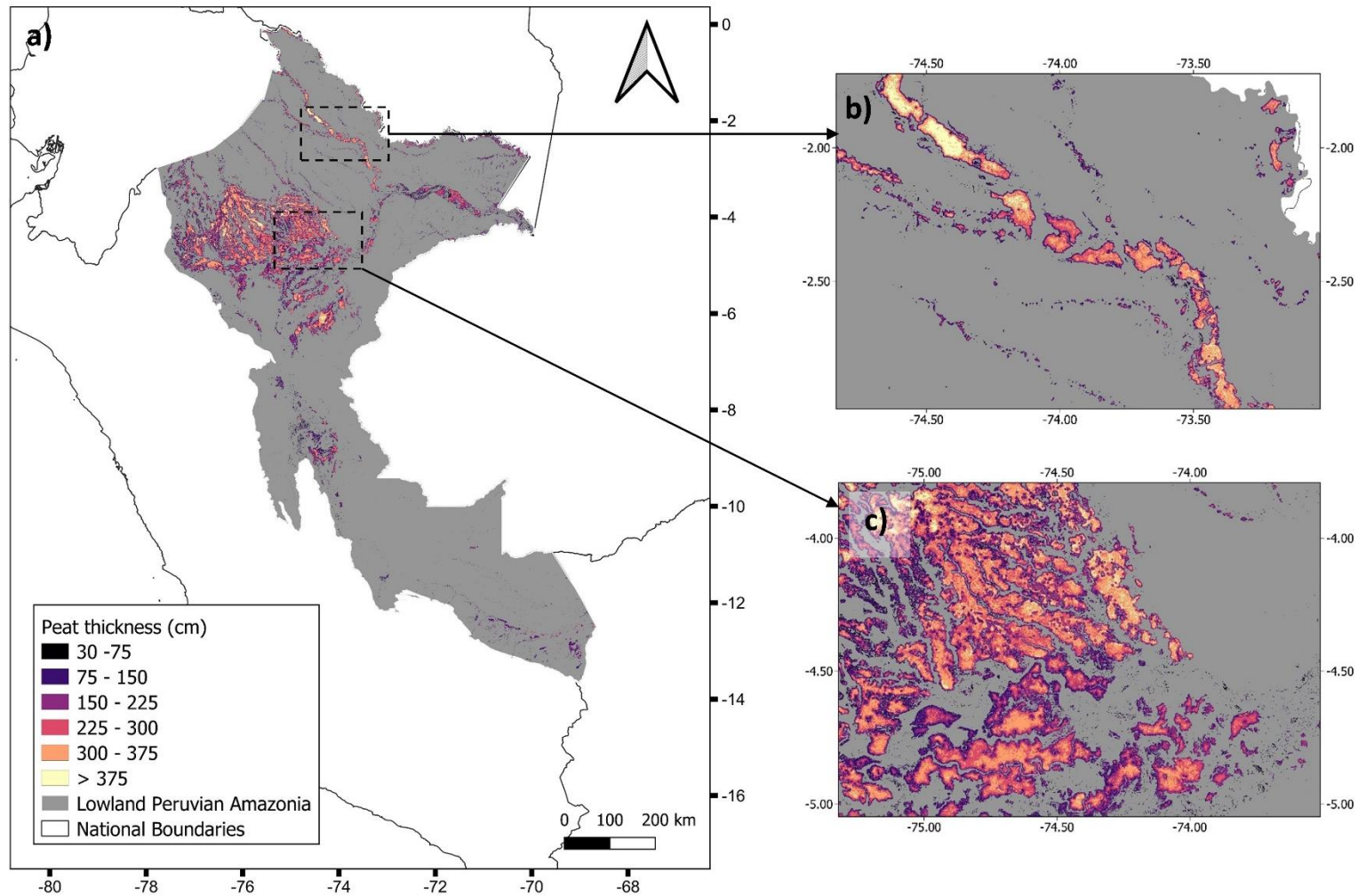
152

153

154

155

Accepted manuscript version



156

157 **Figure 2: Distribution of peat thickness.** a, predicted distribution of peat thickness across lowland Peruvian Amazonia estimated using random forest
 158 regression in Google Earth Engine (median of 1,000 k-folds). b, enlargement showing the Napo River. c, enlargement showing the Marañón and Tigre rivers.
 159 All maps were produced at a resolution of c. 100 m.

160 ***CO₂ emissions from land-use change are small but growing***

161 Our analysis of land-use change data shows that a total peatland area of 1,052 km² was
162 drained and/or cleared during 2000–2005, increasing to 1,667 km² by 2013–2016 (Table 1).
163 Annual emissions from peat decomposition also increased from 3.26 million Mg CO₂ y⁻¹ in
164 2000–2005 to 5.11 million Mg CO₂ y⁻¹ in 2013–2016, while total estimated emissions
165 accounted for 63.83 million Mg CO₂ during the period 2000–2016 mainly due to
166 deforestation (Fig. 3b1, 3b2). Our analysis suggests rapid increases in CO₂ emissions from
167 conversion to mining, urban areas and agriculture, increasing from 2000 to 2016 by 11 times
168 (from 2,426 to 27,634 Mg CO₂ y⁻¹), 9 times (from 2,848 to 26,881 Mg CO₂ y⁻¹) and 5 times
169 (from 77,807 to 411,528 Mg CO₂ y⁻¹), respectively (see Table S4 and S5 for further detail).
170 These estimates exclude emissions from areas where natural peatland vegetation may have
171 been misclassified in 2000 as secondary forest in the land cover dataset Geobosques
172 (amounting to 1,353 km², Table S5). These misclassified areas were revealed by visual
173 inspection of a Google map image of the department of Loreto by someone with local
174 expert knowledge (Fig. 3a).
175 For those areas classified as forest in 2000, as accounted for in Peru's 2016 Forest Reference
176 Emission Level report²⁹, emissions from peat decomposition represent 0.99–3.72% of total
177 national CO₂ emissions from Lowland Peruvian Amazonian forests (i.e. from peat
178 decomposition and biomass loss due to gross deforestation; Table 1).

179

180

181

Table 1: Mean CO₂ emissions from peat decomposition (95% CI) and biomass loss across Lowland Peruvian Amazonia (LPA) for four periods between 2000 to 2016 following Geobosques dataset³⁰. Peat emissions are from this study, biomass emissions are national estimates^a.

	Period			
	2000–2005	2005–2011	2011–2013	2013–2016
Duration (years)	5	6	2	3
Total peatland area with disturbance (km ²)	1,051.63	1,264.50	1,392.82	1,666.76
Total emissions from peat decomposition due to disturbance (x 10 ⁶ Mg CO ₂)	16.29 (6.94, 29.16)	23.27 (9.91, 41.61)	8.95 (3.73, 16.03)	15.33 (6.12, 27.59)
Peatland area with disturbance for categories classified as forest in 2000 (km ²)	158.46	404.38	536.48	808.92
Emissions from peat decomposition due to disturbance for categories classified as forest in 2000 (x 10 ⁶ Mg CO ₂)	1.25 (0.44, 2.25)	5.33 (1.94, 9.55)	2.98 (1.08, 5.35)	6.40 (2.21, 11.59)
Gross deforestation throughout LPA areas classified as forest in 2000 (km ²) ^a	2,483.38	3,945.33	1,915.72	3,303.01
Emissions from biomass loss due to gross deforestation throughout LPA (x 10 ⁶ Mg CO ₂) ^b	124.80	198.65	95.85	165.60
% due to peat decomposition for categories classified as forest in 2000	0.99 (0.35, 1.77)	2.61 (0.97, 4.59)	3.02 (1.12, 5.29)	3.72 (1.32, 6.54)

a 2016 Forest Reference Emission Level report of Peru²⁹.

b CO₂ emission from biomass includes both above- and below-ground biomass of living trees as calculated in the 2016 Forest Reference Emission Level report of Peru²⁹.

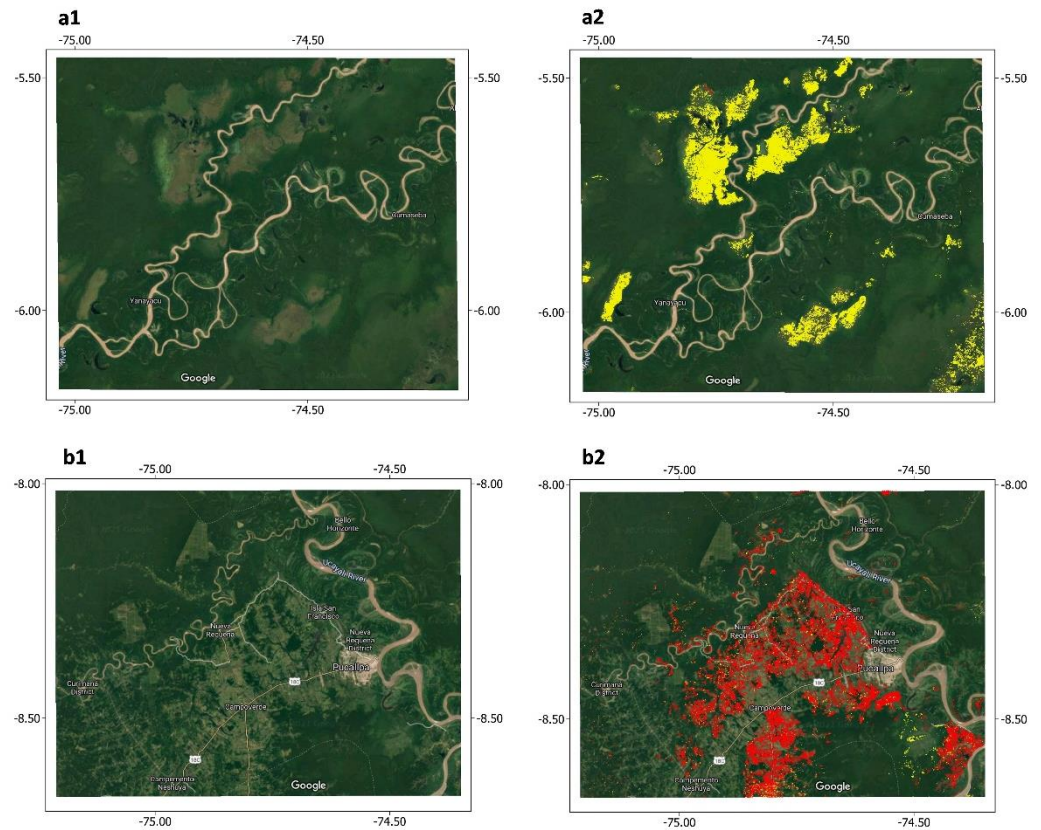
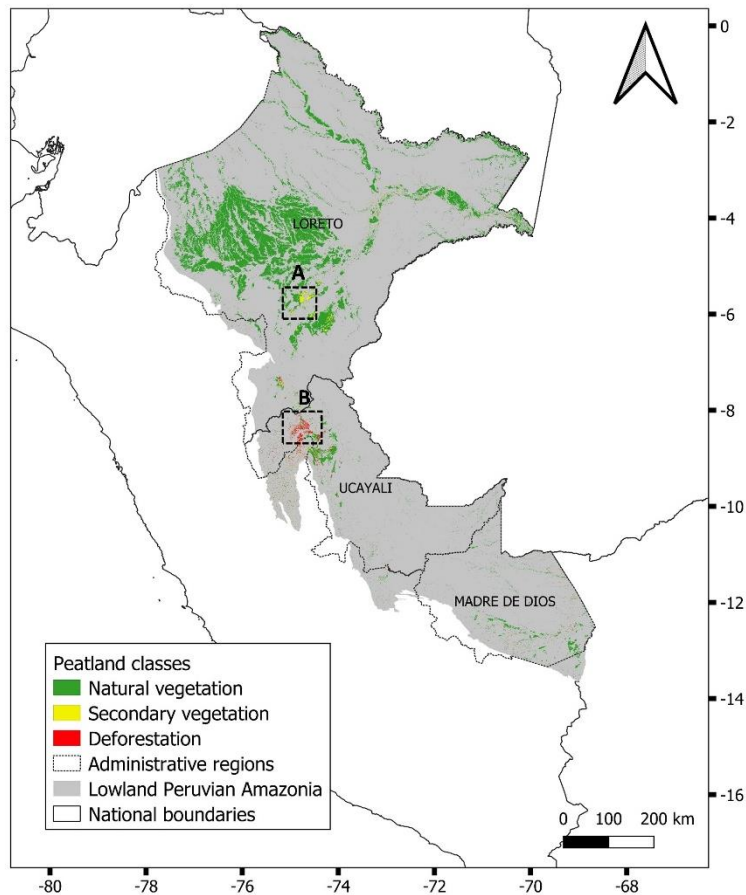
182

183

184

185

186



187

188 **Figure 3: Distribution of peatlands classified as natural vegetation, secondary vegetation and deforestation based on the 2016 forest land and land use**
 189 **categories within Geobosques³⁰ in lowland Peruvian Amazonia.** Non-peatland areas are shown in grey, and the relevant departments of Peru are labelled
 190 within the study area. Google map images show examples of (A) natural peatland vegetation misclassified as secondary forest (shown in a1, a2) around the
 191 Puinahua channel and the Ucayali river in the department of Loreto and (B) peatland areas correctly classified as deforestation (shown in b1, b2) near
 192 Pucallpa in the department of Ucayali.

193 ***Synthesis and future directions***

194

195 Our estimate of the total below-ground carbon stock of 5.38 (2.55–10.58) Pg C across the
196 LPA is 75% of a recent estimate of the entire above-ground C stock of Peru³¹, and
197 approximately doubles previous estimates of the Peruvian tropical peat stock calculated for
198 the PMFB and the MDD regions only^{2,19,22}. Our maps are driven by intensive field sampling
199 which has, for the first time, generated peat thickness data widely across LPA, and which
200 confirms that significant peatlands extend far beyond the relatively well-studied PMFB.

201 Across the main peat-forming landcover classes of pole forest, open peatland and palm
202 swamp, above-ground carbon densities (Table S2,²³) are an order of magnitude lower than
203 respective peat carbon densities, totalling 0.45 Pg C (Table S2). Summing the above- and
204 below-ground carbon stocks gives a central estimate of 5.83 Pg C stored in LPA peatlands.

205 The quantitative uncertainties around the peatland carbon stock are reduced compared to
206 previous studies despite our study covering an area > 5 times greater^{2,22}. Future
207 improvement may be gained by collecting field data where they are still lacking, notably the
208 northwest PMFB and parts of the Ucayali (e.g. around Pucallpa) and Morona basins. Unlike
209 previous studies^{2,22} our study placed no constraints on which landcover classes peat can
210 form under, and we predict that around 2% of seasonally flooded forest is underlain by
211 peat. This suggests that the search for peat should not be solely limited to the well-known
212 peat-forming vegetation types of palm swamp, pole forest and open peatland. In addition to
213 landcover classification maps, we recommend that future fieldwork is informed by
214 examining maps and remote sensing imagery related to hydrology and inundation, such as
215 height above nearest drainage (HAND)³², normalized difference water index (NDWI)³³ and
216 ALOS-PALSAR³⁴ (where possible multi-temporal images).

217 Our approach is driven by remote sensing layers with global coverage and can thus be
218 readily adapted to other regions, provided sufficient field data are available for calibration
219 and validation. Our results call for caution in treating all tropical peatlands as similar, and
220 demonstrate the importance of field data. For example, distance to peatland edge has been
221 found to correlate with peat thickness in other regions such as the Congo basin³, and in
222 most of the basins we studied in Peru. However, we found no significant linear relationship
223 between peat thickness and distance to peatland edge for the data in the MDD basin ($p >$
224 0.1 , $R^2 = 0.005$, Fig. S6c). Householder et al.¹⁹ suggest that this may be because of specific
225 geological conditions in this region: many of the deepest peats in the MDD are often located
226 adjacent to upland (*terra firme*) terraces, close to the peatland edge. This means that the
227 relationship between peat thickness and distance to peatland edge is more complex in MDD
228 than in other regions. Past research points to geomorphological differences between
229 northern and southern parts of Peruvian Amazonia³⁵: while floodplains in northern
230 Amazonia are often wide, rivers in southern Amazonia more often have narrow floodplains
231 confined by terraces. We recommend that new transects should aim to target a range of
232 landscape types (e.g. based on elevation maps) and where possible should cover the full
233 cross-section of each individual peatland. In spite of this limitation, our random forest
234 regression model for the MDD region performs reasonably well.

235 This study assesses CO₂ emissions resulting from peat decomposition due to land-cover
236 change in Peru. Our results suggest that land cover change in the peatlands of the LPA has
237 thus far been restricted to a few hotspot areas, with the largest area of deforestation
238 identified near Pucallpa in the department of Ucayali, an area where recent ground
239 observations confirm the presence of deforested peatlands (²⁶; E. Honorio, pers. comm.).
240 Access to these peatlands has been facilitated by the development of roads and the

241 increasing demand for land for commercial plantations (e.g. oil palm and rice^{36,37}, D. Garcia-
242 Soria, pers. comm.). Overall, the estimated emissions from peat decomposition remain low
243 in Peru but our analysis suggests that the annual emissions are increasing. These findings
244 have two implications for the conservation of these ecosystems. Firstly, the low current
245 emissions support the view that the extensive peatland complex of the LPA is an
246 emblematic example of hydrologically intact moist tropical forest with high structural
247 integrity and therefore should be a high conservation priority^{23,38,39}. Investment is required
248 to promote protection and sustainable management of these widespread and extremely
249 carbon-dense ecosystems, before emissions rise over the coming decades^{40,41}. Secondly, the
250 increasing threats and rising emissions from specific land-use transitions in some peatlands
251 mean that it is important to improve detection of deforestation and secondary vegetation
252 across the full range of peatland forest types, and to make more extensive measurements of
253 greenhouse gas emissions associated with specific land-use transitions across the different
254 forest types^{7,8,9}.

255 Taken together, our results indicate a carbon stock within the peatlands of LPA which is
256 three-quarters as large as the entire above-ground carbon stock of Peru³¹ but contained
257 within just 5% of its land area. The peatlands also contribute substantial ecosystem and
258 floristic diversity to the Amazon^{42,43}. While our study indicates that these peatlands remain
259 largely intact, they face varied and growing threats^{15,37}. Our mapping and carbon stock
260 estimates may be used to support the implementation and enforcement of recent
261 legislation aimed at reducing emissions²⁷ and should act to encourage national and
262 international investment in monitoring, protection and sustainable management of Peru's
263 peatlands, in order that they avoid a similar fate to the heavily degraded peatlands of
264 Southeast Asia³⁷.

265 **Corresponding author**

266 Correspondence to Adam Hastie.

267 **Acknowledgments**

268 This work was funded by NERC (Grant ref. NE/R000751/1)- I.T.L, A.H, K.H.R, E.T.A.M, C.M.A, T.R.B,
269 G.D, E.C.D.G; Leverhulme Trust (Grant ref. RPG-2018-306)-K.H.R, L.E.S.C, C.E.W; Gordon and Betty
270 Moore Foundation (Grant #5439, MonANPeru network)-T.R.B, E.N.H.C, G.F; Wildlife
271 Conservation Society-E.N.H.C; Concytec/British Council/Embajada Británica Lima/Newton
272 Fund (Grant ref. 220-2018)-E.N.H.C, J.D; Concytec/NERC/Embajada Británica Lima/Newton
273 Fund (Grant ref. 001-2019)-E.N.H.C, N.D; the governments of the United States of America
274 (Grant No. MTO-069018) & Norway (Grant Agreement No. QZA-12/0882)-K.H; and NERC
275 Knowledge Exchange Fellowship (Grant Ref No. NE/V018760/1)-E.N.H.C. We thank SERNANP,
276 SERFOR and GERFOR for providing research permits, and the different indigenous and local
277 communities, research stations and tourist companies for giving consent and allowing
278 access to the forests. We acknowledge the invaluable support of technicians Julio Irarica,
279 Julio Sanchez, Hugo Vásquez and Rider Flores, without whom much of the field work would
280 not have been possible. For the purpose of open access, the author has applied a 'Creative
281 Commons Attribution (CC BY) licence to any Author Accepted Manuscript version arising.

282 **Author Contributions**

283 A.H, I.T.L, E.N.H.C, E.T.A.M, K.H.R, T.R.B, L.E.S.C and C.E.W all contributed to the conception,
284 development and design of the study. A.H and E.N.H.C performed the analysis with input
285 from E.T.A.M, K.H, I.T.L, L.E.S.C and P.R.V. A.H and E.N.H.C wrote the manuscript with input

286 from all co-authors. New field data was collected by J.R, A.H, C.M.A, I.T.L, L.E.S.C, C.E.W,
287 N.D, C.J.C-O, G.D, J.D.A, G.F, D.R, and J.G. E.H, O.L, F.D, J.P.J and M.T provided data.

288 **Competing Interests**

289 The authors declare no competing interests

290 **References**

291

- 292 1. Dommain, R., Couwenberg, J. & Joosten, H. Development and carbon sequestration
293 of tropical peat domes in south-east Asia: links to post-glacial sea-level changes and
294 Holocene climate variability. *Quat. Sci. Rev.* **30**, 999–1010 (2011).
- 295 2. Draper, F. C. *et al.* The distribution and amount of carbon in the largest peatland
296 complex in Amazonia. *Environ. Res. Lett.* **9**, 124017 (2014).
- 297 3. Dargie, G. C. *et al.* Age, extent and carbon storage of the central Congo Basin
298 peatland complex. *Nature* **542**, 86 (2017).
- 299 4. Ribeiro, K. *et al.* Tropical peatlands and their contribution to the global carbon cycle
300 and climate change. *Glob. Chang. Biol.* **27**, 489–505 (2021).
- 301 5. Wang, S., Zhuang, Q., Lähteenoja, O., Draper, F. C. & Cadillo-Quiroz, H. Potential shift
302 from a carbon sink to a source in Amazonian peatlands under a changing climate.
303 *Proc. Natl. Acad. Sci.* **115**, 12407–12412 (2018).
- 304 6. IPCC. *2013 Supplement to the 2006 IPCC Guidelines for National Greenhouse Gas*
305 *Inventories: Wetlands. Prepared by Hiraishi, T., Krug, T., Tanabe, K., Srivastava, N.,*
306 *Baasansuren, J., Fukuda, M. and Troxler, T.G. (eds).* (2014).

- 307 7. van Lent, J., Hergoualc'h, K., Verchot, L., Oenema, O. & van Groenigen, J. W.
308 Greenhouse gas emissions along a peat swamp forest degradation gradient in the
309 Peruvian Amazon: soil moisture and palm roots effects. *Mitig. Adapt. Strateg. Glob.
310 Chang.* **24**, 625–643 (2019).
- 311 8. van Lent, J. Land-use change and greenhouse gas emissions in the tropics: Forest
312 degradation on peat soils. PhD dissertation, Wageningen University. (2020).
- 313 9. Hergoualc'h, K. *et al.* Spatial and temporal variability of soil N₂O and CH₄ fluxes along
314 a degradation gradient in a palm swamp peat forest in the Peruvian Amazon. *Glob.
315 Chang. Biol.* **26**, 7198–7216 (2020).
- 316 10. Swails, E., Hergoualc'h, K., Verchot, L., Novita, N. & Lawrence, D. Spatio-Temporal
317 Variability of Peat CH₄ and N₂O Fluxes and Their Contribution to Peat GHG Budgets in
318 Indonesian Forests and Oil Palm Plantations. *Front. Environ. Sci.* **9**, 48 (2021).
- 319 11. Gaveau, D. L. A. *et al.* Major atmospheric emissions from peat fires in Southeast Asia
320 during non-drought years: evidence from the 2013 Sumatran fires. *Sci. Rep.* **4**, 6112
321 (2014).
- 322 12. Page, S. E. *et al.* The amount of carbon released from peat and forest fires in
323 Indonesia during 1997. *Nature* **420**, 61–65 (2002).
- 324 13. Mishra, S. *et al.* Degradation of Southeast Asian tropical peatlands and integrated
325 strategies for their better management and restoration. *J. Appl. Ecol.* **58**, 1370–1387
326 (2021).
- 327 14. Dargie, G. C. *et al.* Congo Basin peatlands: threats and conservation priorities. *Mitig.
328 Adapt. Strateg. Glob. Chang.* **24**, 669–686 (2019).

- 329 15. Roucoux, K. H. *et al.* Threats to intact tropical peatlands and opportunities for their
330 conservation. *Conserv. Biol.* **31**, 1283–1292 (2017).
- 331 16. Griscom, B. W. *et al.* Natural climate solutions. *Proc. Natl. Acad. Sci.* **114**, 11645–
332 11650 (2017).
- 333 17. Girardin, C.A.J., Jenkins, S., Seddon, N., Allen, M., Lewis, S.L., Wheeler, C.E., Griscom,
334 B.W. & Malhi, Y. . Nature-based solutions can help cool the planet — if we act now.
335 *Nature* **593**, 191–194 (2021).
- 336 18. Murdiyarso, D., Lilleskov, E. & Kolka, R. Tropical peatlands under siege: the need for
337 evidence-based policies and strategies. *Mitig. Adapt. Strateg. Glob. Chang.* **24**, 493–
338 505 (2019).
- 339 19. Householder, J. E., Janovec, J. P., Tobler, M. W., Page, S. & Lähteenoja, O. Peatlands
340 of the Madre de Dios River of Peru: Distribution, Geomorphology, and Habitat
341 Diversity. *Wetlands* **32**, 359–368 (2012).
- 342 20. Hess, L. L. *et al.* Wetlands of the Lowland Amazon Basin: Extent, Vegetative Cover,
343 and Dual-season Inundated Area as Mapped with JERS-1 Synthetic Aperture Radar.
344 *Wetlands* **35**, 745–756 (2015).
- 345 21. Gumbrecht, T. *et al.* An expert system model for mapping tropical wetlands and
346 peatlands reveals South America as the largest contributor. *Glob. Chang. Biol.* **23**,
347 3581–3599 (2017).
- 348 22. Lähteenoja, O. *et al.* The large Amazonian peatland carbon sink in the subsiding
349 Pastaza-Marañón foreland basin, Peru. *Glob. Chang. Biol.* **18**, 164–178 (2012).
- 350 23. Coronado, E. N. H. *et al.* Intensive field sampling increases the known extent of

- 351 carbon-rich Amazonian peatland pole forests. *Environ. Res. Lett.* **16**, 74048 (2021).
- 352 24. Hergoualc'h, K., Gutiérrez-Vélez, V. H., Menton, M. & Verchot, L. V. Characterizing
353 degradation of palm swamp peatlands from space and on the ground: An exploratory
354 study in the Peruvian Amazon. *For. Ecol. Manage.* **393**, 63–73 (2017).
- 355 25. Baker, T.R., del Castillo Torres, D., Honorio Coronado, E., Lawson, I., Brañas, M.M.,
356 Montoya, M., Roucoux, K. The challenges for achieving conservation and sustainable
357 development within the wetlands of the Pastaza Marañón basin, Peru. pp. 155-175 in
358 'Peru: Deforestation in times of climate change' (ed. A. Chirif), *International Work*
359 *Group for Indigenous Affairs*,. (2019).
- 360 26. López Gonzales, M.; Hergoualc'h, K.; Angulo Núñez, Ó.; Baker, T.; Chimner, R.; del
361 Águila Pasquel, J.; del Castillo Torres, D.; Freitas Alvarado, L.; Fuentealba Durand, B.;
362 García Gonzales, E.; Honorio Coronado, E.; Kazuyo, H.; Lilleskov, E.; Málaga Durán, F.
363 What do we know about Peruvian peatlands? Bogor, Indonesia. Retrieved from
364 https://www.cifor.org/publications/pdf_files/OccPapers/OP-210.pdf (2020).
- 365 27. MINAM. Decreto Supremo N° 006-2021-MINAM (2021).
- 366 28. Lähteenoja, O., Ruokolainen, K., Schulman, L. & Oinonen, M. Amazonian peatlands:
367 an ignored C sink and potential source. *Glob. Chang. Biol.* **15**, 2311–2320 (2009).
- 368 29. MINAM. Peru's submission of a Forest Reference Emission Level (FREL) for reducing
369 emissions from deforestation in the Peruvian Amazon. 77 pages (2016).
- 370 30. MINAM. *Coberturas de uso y cambio de uso de la tierra para los periodos 2000-2005,*
371 *2005-2011, 2011-2013, 2013-2016. Monitoreo de los cambios sobre la cobertura de*
372 *los bosques peruanos – Geobosques.* (2020).

- 373 31. Csillik, O., Kumar, P., Mascaro, J., O’Shea, T. & Asner, G. P. Monitoring tropical forest
374 carbon stocks and emissions using Planet satellite data. *Sci. Rep.* **9**, 17831 (2019).
- 375 32. Donchyts, Gennadii., Winsemius, Hessel., Schellekens, Jaap., Erickson, Tyler., Gao,
376 Hongkai., Savenije, Hubert., and van de Giesen, N. ‘Global 30m Height Above the
377 Nearest Drainage (HAND)’. in (Geophysical Research Abstracts, Vol. 18, EGU2016-
378 17445-3, 2016, EGU General Assembly, 2016).
- 379 33. Drusch, M. *et al.* Sentinel-2: ESA’s Optical High-Resolution Mission for GMES
380 Operational Services. *Remote Sens. Environ.* **120**, 25–36 (2012).
- 381 34. Shimada, M. *et al.* New global forest/non-forest maps from ALOS PALSAR data (2007–
382 2010). *Remote Sens. Environ.* **155**, 13–31 (2014).
- 383 35. Toivonen, T., Mäki, S. & Kalliola, R. The riverscape of Western Amazonia – a
384 quantitative approach to the fluvial biogeography of the region. *J. Biogeogr.* **34**,
385 1374–1387 (2007).
- 386 36. Vijay, V., Reid, C. D., Finer, M., Jenkins, C. N. & Pimm, S. L. Deforestation risks posed
387 by oil palm expansion in the Peruvian Amazon. *Environ. Res. Lett.* **13**, 114010 (2018).
- 388 37. Lilleskov, E. *et al.* Is Indonesian peatland loss a cautionary tale for Peru? A two-
389 country comparison of the magnitude and causes of tropical peatland degradation.
390 *Mitig. Adapt. Strateg. Glob. Chang.* **24**, 591–623 (2019).
- 391 38. Watson, J. E. M. *et al.* The exceptional value of intact forest ecosystems. *Nat. Ecol.*
392 *Evol.* **2**, 599–610 (2018).
- 393 39. Hansen, A. J. *et al.* A policy-driven framework for conserving the best of Earth’s
394 remaining moist tropical forests. *Nat. Ecol. Evol.* **4**, 1377–1384 (2020).

- 395 40. Maxwell, S. L. *et al.* Degradation and forgone removals increase the carbon impact of
396 intact forest loss by 626%. *Sci. Adv.* **5**, 10 (2019).
- 397 41. Grantham, H. S. *et al.* Anthropogenic modification of forests means only 40% of
398 remaining forests have high ecosystem integrity. *Nat. Commun.* **11**, 5978 (2020).
- 399 42. Lähteenoja, O. & Page, S. High diversity of tropical peatland ecosystem types in the
400 Pastaza-Marañón basin, Peruvian Amazonia. *J. Geophys. Res. Biogeosciences* **116**,
401 (2011).
- 402 43. Draper, F. C. *et al.* Peatland forests are the least diverse tree communities
403 documented in Amazonia, but contribute to high regional beta-diversity. *Ecography*,
404 **41**, 1256–1269 (2018).

405

406

407 **Methods**

408 ***Fieldwork***

409 Between 2019 and 2021, we collected 445 new ground reference points (GRPs) within LPA
410 (Fig. 1, 294 of which were presented by ref.²³) collecting data on the substrate (i.e. peat
411 thickness, where peat is present) and vegetation type (e.g. palm swamp). We focused data
412 collection on regions with no existing GRPs, where peat was believed to be present based
413 on remote sensing imagery (e.g. various Landsat 8 [Fig. S7] and Sentinel 2 bands), including
414 the Napo, Putumayo, Tapiche and Tigre river basins (Fig. 1, Fig. S1), using the only available
415 means of access, i.e. via rivers and streams. We also collected new data on peat thickness
416 and carbon concentration from under-sampled peatland ecosystems (e.g. peatland pole

417 forest). We made the sampling as spatially representative as possible within the constraints
418 of logistical feasibility, personal safety and accessibility, which are substantial in these
419 remote regions of Peru. The previously published datasets which we incorporated here
420 were also subject to the same constraints.

421 Where present, peat thickness was measured with an auger or Russian-type peat corer,
422 either along transects perpendicular to the river at intervals of 200–500 m, or at the four
423 corners and centre of the vegetation plots (see below) in which case the value for peat
424 thickness used is the mean of five point measurements. Working along transects leading
425 away from the river and into the peatlands allowed us to sample across wide hydrological
426 and topographic gradients, including both minerotrophic and ombrotrophic ecosystems. At
427 91 of these GRPs, we conducted 1 ha, 0.5 ha or 0.1 ha vegetation plot surveys (collecting
428 floristic data) for quantitative classification of ecosystem type^{23,43}. Additionally, we used 218
429 previously published GRPs^{2,22,28} (24 with floristic data) collected using a similar transect-
430 based sampling strategy in northern Peru and 465 GRPs¹⁹ (148 with floristic data) collected
431 in southern Peru, amounting to a total of 1,128 GRPs (Fig. 1). Of these, 887 GRPs (Fig. S8)
432 indicated the presence of peat (defined as an organic layer ≥ 30 cm thick⁴⁴). Two examples
433 of peat thickness measurement transects in the Napo basin are shown in Figure S7.

434 The majority of peat thickness observations do not have corresponding carbon
435 concentration measurements and thus we cannot enforce a precise cut-off in terms of
436 carbon content. However, we visually identified peat and underlying sediments in the field
437 on the basis of their physical properties (e.g. colour, structure, texture) and composition
438 (e.g. wood, roots, mineral components)^{45,46}. At 35 vegetation plots identified by
439 fieldworkers as being on peat, we took sediment samples in the near-basal peat, transition

440 zone and underlying mineral sediment (typically silts or clays) and measured loss on ignition
441 (LOI) in each to test the visual assessments. The peat, transition zone and mineral samples
442 had mean LOI values of 70%, 28% and 13% respectively (see Table S6). This gives us
443 confidence that fieldworkers in this region are able to visually identify peat (in this case, soil
444 with an LOI of at least 50%), as there is typically a clear and distinct transition to mineral
445 sediment in Peruvian peatlands.

446 ***Map of predicted peatland extent in lowland Peruvian Amazonia***

447 We created a 50 m resolution map (Fig. S2) of predicted peatland extent in LPA (defined
448 here as the area covered by two of the ecozones recognized by Peru's Ministry of
449 Environment: Ecozone Selva Baja and Ecozone Hidromórfica⁴⁷). Firstly, we ran a supervised
450 random forest (RF) algorithm (200 trees) in Google Earth Engine to predict the distribution
451 of five classes: peat below forest (PBF), peat below non-forest (i.e. herbaceous vegetation
452 and shrubland, PBNF), non-peat below forest (NBF), non-peat below non-forest (NBN) and
453 open water (WA). The model was trained and validated (50/50 split of polygons) using peat
454 thickness measurements and information on the overlying vegetation, and driven using a
455 stack of seven remote sensing layers including two Sentinel-2 indices (NDVI & NDWI³³),
456 three ALOS PALSAR-2 bands (HH, HV, HH/HV³⁴), SRTM 30 m digital elevation⁴⁸ (Table S7),
457 and an extended version of a landcover classification produced previously²³ (Fig. S9;
458 Supplementary Information has further details). The PBF and PBNF categories were
459 amalgamated to form the map of total peatland extent in Fig. S2. We calculated 5th and 95th
460 confidence interval percentiles for peatland area using the area and accuracy of each class,
461 applying the method described in ref. ⁴⁹ (equations 9–13), following ref. ² and
462 recommended by the Global Forest Observations Initiative.

463 **Model of peat thickness distribution**

464 Testing showed that peat thickness increases with distance to peatland edge ($R^2 = 0.13$, $p <$
465 0.0001 , Fig. S6), indicating that the deepest peat is typically found in the centre of a
466 peatland. We thus calculated distance to peatland edge for each model grid, using our map
467 of peatland extent. We used the 1,128 peat thickness measurements as training data,
468 supplemented with points that we assumed to lack peat located along known rivers and
469 urban areas (based on a combination of local knowledge and inspection of Sentinel-2 and
470 Landsat 8 images), amounting to a final dataset of 1,359 points. The model was run at 100 m
471 resolution in Google Earth Engine and driven by the stack of remote sensing layers, with two
472 additional layers: distance to peatland edge, and height above nearest drainage (HAND³²)
473 (Table S8).

474 In order to robustly test model performance, we performed a series of validations which
475 accounted for spatial autocorrelation. Training the model using data only from within the
476 PMFB ($n = 717$) and testing against data from outside the PMFB in Northern Peru (Napo,
477 Putumayo and upper Amazon basins, $n = 155$), the model performed relatively well
478 (Observed vs Predicted peat thickness, $p < 0.0001$; $R^2 = 0.56$, Fig. S10a). However, the same
479 model (trained using only PMFB data) was unable to predict variation in peat thickness
480 observed in the Madre De Dios (MDD) basin data ($n = 478$, $p > 0.50$; $R^2 = 0.00$, Fig. S10b). For
481 this reason, we decided to run two separate models for the final analysis, one using data
482 only within the MDD basin ($n = 477$, no. model trees = 100), and another using all other data
483 points ($n = 867$, no. model trees = 50). Model performance was lower in the model which
484 used only MDD data ($p < 0.0001$; $R^2 = 0.38$, RMSE = 70%, Fig. S5b) than that using all other
485 data points (Observed Vs Predicted peat thickness, $p < 0.0001$; $R^2 = 0.66$, RMSE = 66%, Fig.

486 S5a). We independently validated both models by training each with 80% of the data
487 (randomly selected) and testing with the remaining 20% (Fig. S5c, d).

488 To account for the uncertainty associated with our estimate of peat thickness distribution,
489 we ran a k-fold analysis as in⁵⁰, splitting the data into 1,000 folds, and therefore generating
490 1,000 predictions of peat thickness per pixel. We took the median, 5th and 95th percentiles
491 of the 1,000 predictions to represent our best estimate (Fig. 2a), minimum (Fig. S3a) and
492 maximum (Fig. S3b) peat thickness distributions. We subsequently masked the maps of peat
493 thickness distribution using the map of peatland extent (Fig. S2), thus restricting our model
494 to only regions predicted to contain peat.

495 ***Below-ground carbon stock***

496 A dataset of 68 stratigraphic profiles of carbon concentration (%) and dry bulk density (DBD,
497 g cm⁻³) was compiled using data from refs^{2,22,23,28,51} (see Table S9). This includes ten new
498 peat profiles collected as part of this study and described in²³ (see Table S4 of Honorio
499 Coronado et al., 2021²³). We calculated peat carbon stock (PC, Mg C ha⁻¹) from the peat
500 cores by multiplying peat thickness (cm) by DBD and carbon concentration evaluated at
501 regular intervals down the peat profile to the base of the peat. Laboratory conditions varied
502 depending on the study and can be found in the original papers, along with information on
503 protocols. The studies used a variety of standard methodologies to determine sample
504 carbon concentrations. In line with our definition of peat, we only retained cores in which
505 the peat was ≥ 30 cm thick, with a mean LOI of $\geq 50\%$, and those collected using a Russian
506 corer to ensure that DBD measurements were based on a reliable volumetric sample.

507 We performed a sensitivity analysis to test which of the three components of PC (i.e. peat
508 thickness, DBD and carbon concentration) was most important. Peat thickness was found to

509 be the most important determinant of total PC ($p < 0.0001$; $R^2 = 0.81$, Fig. S11). We thus
510 used our model of peat thickness distribution to estimate total PC for each 100 m grid-cell
511 and then summed across the entire LPA to produce a total value for the peat carbon stock.
512 In order to produce uncertainty bounds for our estimate of the total peat C stock, we ran a
513 Monte Carlo analysis which accounted for the uncertainty in each stage of our
514 methodology. We ran 1,000 simulations for PC, constrained using the standard error of the
515 b-estimates from the regression equation (peat thickness vs PC, Fig. S11). This was
516 performed twice, once using the 5th and then the 95th percentile distribution of peat
517 thickness calculated previously (Fig. S3). These 1,000 PC simulations were in turn multiplied
518 by 1,000 simulations of peatland area per grid, constrained by the confidence intervals
519 calculated previously. Finally, the maps of the 5th and 95th percentile of peat C stock per grid
520 were summed across LPA to derive the final minimum and maximum uncertainty bounds.

521

522 ***Activity data and emissions from peat decomposition***

523 To estimate changes in forest cover, we used reports of activity data provided by Peru's
524 national monitoring platform, Geobosques³⁰. These reports were generated using Landsat 7
525 and 8 images from 2001 to 2016 at 30 m resolution, with cumulative areas of different land
526 uses for the year 2000³⁰. In these data, Peruvian Amazonia is classified into 11 land uses for
527 the periods 2000–2005, 2005–2011, 2011–2013, and 2013–2016. Figure 3 shows our
528 predicted peatland map (produced by re-running our model at 30 m resolution to match the
529 activity dataset) grouping the categories that represent natural vegetation (forest, forest on
530 wetland, wet savannah, water body, non-forest on wetland), secondary vegetation, and
531 deforested areas (agriculture, pasture, urban areas, mining areas, bare ground).

532 Emission factors for organic soils were taken from Chapter 2 of the 2013 Supplement to the
533 2006 IPCC Guidelines for the National GHG Inventory for Wetlands⁶. The values range from
534 7.5 Mg C ha⁻¹ y⁻¹ for secondary vegetation to 9.6 Mg C ha⁻¹ y⁻¹ for deforested peatlands
535 (Table S4). These IPCC values are intended to be used for drained peatlands, but peatland
536 disturbance in Peru does not necessarily entail drainage. Nonetheless, undrained secondary
537 forests on peat in Indonesia lose soil carbon (1.4 Mg C ha⁻¹ y⁻¹; ¹⁰) at a similar rate to
538 shallow-drained plantations (1.5 Mg C ha⁻¹ y⁻¹; ⁶), and CO₂ emissions in highly degraded
539 undrained peatlands in Peru (e.g. degraded *Mauritia*-dominated palm swamps classified as
540 secondary vegetation: 7.1 Mg C ha⁻¹ y⁻¹; ⁸) fall within the range of the values of deforested
541 drained peatlands in Indonesia (1.5–14.0 Mg C ha⁻¹ y⁻¹; ⁶, Table S5). Therefore, we assume
542 the IPCC emission factors are acceptable estimates for drained or undrained peatlands in
543 Peru, which is reasonable given that it matches the available evidence.

544 Total CO₂ emissions following land use change due to inferred peat decomposition were
545 estimated following the equation 2.3 from Chapter 2 in the IPCC Wetlands Supplement⁶:

546

$$547 \quad PDE = \sum_{ij=0}^n A_{ij} * EF_{ij} * t * 44/12 \quad (1)$$

548

549 Where *PDE* is total CO₂ emissions from peat decomposition (Mg CO₂); *A* is the area (ha) on
550 peatlands of the original land-use category-*i* that was converted into category-*j* during the
551 time period *t* (years); *EF* is the mean annual emission factor of peat decomposition assigned
552 to the conversion from category-*i* to category-*j* (Mg C ha⁻¹ y⁻¹) and converted to CO₂ by
553 multiplying by the atomic mass factor of 44/12 ^{52,53}. For example, within peatlands
554 (according to our map), forest on wetland (ecosystem saturated with water and assumed

555 zero CO₂ emissions) that is converted to mining area (ecosystem assumed similar to drained
556 grasslands with emissions of 9.6 Mg C ha⁻¹ y⁻¹) will receive an *EF* value of 4.8 Mg C ha⁻¹ y⁻¹
557 following⁵² (Table S5).

558

559

560 **Data availability**

561 An interactive map of modelled peatland extent (50 m resolution) can be viewed here:

562 <https://code.earthengine.google.com/a07b25e62adbe714afa77e4a3e423b1b>

563 and source map downloaded here:

564 An interactive map of modelled landcover class (50 m resolution) can be viewed here:

565 <https://code.earthengine.google.com/f3a655bbf36db6121be1d7fd09991530>

566 and source map downloaded here: <https://datashare.ed.ac.uk/handle/10283/4364>

567 An interactive map of modelled peat thickness distribution (100 m resolution) can be

568 viewed here: <https://code.earthengine.google.com/8845760a7e086df8b1e66075985ea705>

569 and source maps downloaded here: <https://datashare.ed.ac.uk/handle/10283/4364>

570 An interactive map of modelled peat carbon (100 m resolution) can be viewed here:

571 <https://code.earthengine.google.com/394ed8b119c1913f7c5f5b6a969ec19f>

572 and source maps downloaded here: <https://datashare.ed.ac.uk/handle/10283/4364>

573 The MINAM Geobosques³⁰ raster file can be downloaded here:

574 <https://geobosques.minam.gob.pe/geobosque/view/descargas.php?122345gx345w34gg>

575

576 **Code availability**

577 The above Google Earth Engine links include code for some basic analysis of the maps. Code

578 for other parts of the analysis will be made available upon reasonable request to the

579 corresponding author.

580

581 **Additional references for methods**

582

583 44. Page, S. E., Rieley, J. O. & Banks, C. J. Global and regional importance of the tropical

584 peatland carbon pool. *Glob. Chang. Biol.* **17**, 798–818 (2011).

- 585 45. Troels-Smith, J. Characterisation of unconsolidated sediments. *Danmarks Geol.*
586 *Undersogelse IV*, 73 (1955).
- 587 46. Kershaw., A. . A modification of the Troels-Smith system of sediment description and
588 portrayal. *Quat. Australas.* **15**, 63–68 (1997).
- 589 47. Málaga, N., Giudice, R., Vargas, C., y Rojas, E. *Estimación de los contenidos de carbono*
590 *de la biomasa aérea en los bosques de Perú.* Lima: Ministerio del Ambiente del Perú.
591 (2014).
- 592 48. Farr, T. G. *et al.* The Shuttle Radar Topography Mission. *Rev. Geophys.* **45**, (2007).
- 593 49. Olofsson, P., Foody, G. M., Stehman, S. V & Woodcock, C. E. Making better use of
594 accuracy data in land change studies: Estimating accuracy and area and quantifying
595 uncertainty using stratified estimation. *Remote Sens. Environ.* **129**, 122–131 (2013).
- 596 50. Rodríguez-Veiga, P. *et al.* Carbon Stocks and Fluxes in Kenyan Forests and Wooded
597 Grasslands Derived from Earth Observation and Model-Data Fusion. *Remote Sensing*
598 vol. 12 (2020).
- 599 51. Bhomia, R. K. *et al.* Impacts of *Mauritia flexuosa* degradation on the carbon stocks of
600 freshwater peatlands in the Pastaza-Marañón river basin of the Peruvian Amazon.
601 *Mitig. Adapt. Strateg. Glob. Chang.* **24**, 645–668 (2019).
- 602 52. Ministry of Environment and Forestry. Indonesia. *MoEF, 2016, National Forest*
603 *Reference Emission Level for Deforestation and Forest Degradation: In the Context of*
604 *Decision 1/CP.16 para 70 UNFCCC (Encourages developing country Parties to*
605 *contribute to mitigation actions in the forest sector), Directorate . (2016).*

606 53. IPCC. *IPCC guidelines for National Greenhouse Gas Inventories. Agriculture, forestry*
607 *and other land use (AFOLU), Vol. 4*, Eggleston, S., L. Buendia, K. Miwa, T. Ngara, and
608 *K. Tanabe (eds.). Prepared by the National Greenhouse Gas Inventories Programme,*
609 *Institu.* <https://www.ipcc-nggip.iges.or.jp/public/2006gl/vol4> (2006).

610

Accepted manuscript version